Cu/SiO_2 CATALYSTS OBTAINED BY CATIONIC ADSORPTION FROM DIFFERENT PRECURSOR SALTS

D.B. TAGUA, E. ALVAREZ ZURBANO, P.M. GÓMEZ LARGO and B.P. BARBERO

Instituto de Investigaciones en Tecnología Química (INTEQUI), UNSL-CONICET.
Facultad de Química, Bioquímica y Farmacia, Universidad Nacional de San Luis.
Almirante Brown 1455, C.P. D5700HGC, San Luis, Argentina.
bbarbero@unsl.edu.ar

***Abstract*— In this work the effect of different copper precursor salts (acetate, nitrate, sulfate) on the physicochemical characteristics of Cu/SiO_2 catalysts is studied. The catalysts were prepared by the cationic adsorption method and analyzed by several characterization techniques (TGA, DSC, FTIR, XRD, AAS, SEM-EDS, N_2-sorptometry and TPR). The results showed that the copper acetate precursor generated highly dispersed nano-sized copper oxide species on the silica surface, while the copper nitrate precursor leaded to bulk-type copper oxide strongly interacting with the silica, and the copper sulfate precursor did not decompose completely during the catalyst preparation. Besides, the acetate precursor produced the highest copper content, due to lower acidity of its solution, which generated a higher density of negative charge on the silica surface and a higher affinity for cupric ions. In conclusion, the great influence of the nature of the precursor salt on the physicochemical characteristics of silica-supported copper catalysts is established.**

***Keywords*— Silica-supported copper, cationic adsorption method, physicochemical characteristics**

I. INTRODUCTION

Copper-based catalysts are widely used in a variety of industrial processes and laboratory-scale studies. Copper can be forming a mixed solid, such as spinels, perovskites, etc., or it can be supported as an oxide on a support material that provides a large surface area and adequate physical structure for its application in catalytic reactors. Cu/SiO_2 catalysts, in particular, have been studied for a wide variety of reactions, such as hydrogenolysis reactions (Aubrecht *et al*., 2022; Zhu *et al.*, 2015), oxalate and aldehyde hydrogenations (Huang *et al.*, 2022; Zhang *et al.*, 2012; Santori *et al.*, 2000), alcohols dehydrogenation (Wang *et al.*, 2003; Guerreiro *et al.*, 2000), CO oxidation (Xi *et al.*, 2014; Hossain *et al.*, 2018), wet phenol oxidation (Zhong *et al.*, 2012), among others.

The catalytic properties of supported copper catalysts are strongly influenced by the synthesis variables. Several researchers had studied the nature of the support used (Aubrecht *et al*., 2022; Hossain *et al.*, 2018), the method of preparation (Aubrecht *et al*., 2022; Wang *et al.*, 2003; Guerreiro *et al.*, 2000), the copper loading in the catalyst (Zhang *et al.*, 2012), and other parameters (Toupance *et al*., 2000; Toupance *et al.*, 2002), demonstrating the effect on the physicochemical characteristics and catalytic behavior.

This work aims to evaluate the influence of different copper precursor salts (acetate, nitrate, sulfate) on the physicochemical characteristics of silica-supported copper catalysts (Cu/SiO_2) when the cationic adsorption method is used for the preparation of the catalysts. The cationic adsorption method is based on the electrostatic interaction of Cu^{2+} cations with the surface charges of the silica support. The difference between the point of zero charge (PZC) of the silica and the pH of the solution containing the copper ions plays a fundamental role in this interaction (Munnik *et al*, 2015). Furthermore, the solution pH is defined by the nature of the anions of the precursor salts, and in this fact lies the importance of this study.

II. METHODS

A. Synthesis of catalysts

The silica support was obtained from a colloidal suspension of commercial SiO_2 NexSil 20 Nyacol®, drying it at 70 °C for 24 hours. Then, the solid was ground and sieved using a mesh ASTM No. 140 (105 micron), and calcined at 300 °C for 2 hours. The catalysts were synthesized by the cationic adsorption method. For this, 0.2 M aqueous solutions of three copper precursor salts were prepared: copper sulfate ($CuSO_4 \cdot 5H_2O$, Biopack), copper nitrate ($Cu(NO_3)_2 \cdot 3H_2O$, Merck) and copper acetate ($C_4H_6CuO_4 \cdot H_2O$, Fluka). In 50 mL of each solution, 5 grams of SiO_2 were added and stirred in ultrasonic bath at room temperature for 30 minutes. Subsequently, the solid was vacuum filtered, dried in microwaves to constant weight and calcined in air at 500 °C for 2 hours. Microwave drying is a rapid method and has been shown to provide a very homogeneous distribution of the active phase in structured catalysts (Martinez *et al.*, 2020). The catalysts obtained were called Cu/SiO_2-α, where α represents the precursor salts: acetate (a), nitrate (n) and sulfate (s).

B. Characterization techniques

Thermogravimetric analyzes (TGA) were performed in a Shimadzu TGA 51 and differential scanning calorimetry (DSC) in a Shimadzu DSC 60, using about 5 mg of sample, a heating speed of 10 °C/min and a 50 mL/min airflow. Fourier Transform Infrared spectra (FTIR) were acquired with a Nicolet Protégé 460 FTIR instrument between 4000 and 250 cm^{-1} using KBr pellets. X-ray diffractograms (XRD) were obtained with a Rigaku ULTIMA IV diffractometer using a copper radiation

source (λ=0.15418 nm) with a nickel filter, operated at 30 kV and 20 mA in the 2θ range from 10º to 70º. The copper content in the catalysts was determined by atomic absorption spectroscopy (AAS) using a Shimadzu model AA-6300 equipment at a wavelength of 324.8 nm, after acid digestion of the catalysts with HF. The catalysts were examined by scanning electron microscopy (SEM) using a LEO 1450 VP microscope coupled to a Genesis 2000 energy dispersive spectrometer (EDS). The nitrogen adsorption-desorption isotherms were acquired in a Micromeritics Gemini V equipment after to degas the samples at 250 ºC; and then, the specific surface areas by BET method (S_{BET}), the pore volume (V_{pore}) and pore mean size (D_{pore}) by BJH method were calculated. The temperature programmed reduction (TPR) experiments were performed in lab-made equipment equipped with temperature and mass flow controllers and a thermal conductivity detector for recording the hydrogen consumption. Typically, 100 mg of catalyst, a heating rate of 10 °C/min from room temperature to 550 °C, and a 5% H_2/N_2 mixture at a flow rate of 30 mL/min were used.

III. RESULTS AND DISCUSSION

Firstly, thermal analyzes (TGA and DSC) of the dry solids were carried out in order to determinate the stability of the copper precursor salts used for the impregnation of the silica (Fig. 1). In all the TGA curves, a mass loss below 150 °C is observed, and it is associated with an endothermic event in the DSC curve, whereby can be attributed to dehydration of the samples. In the case of the catalyst prepared from copper acetate (Fig. 1A), a second mass loss is observed between 275 ºC and 310 ºC, which corresponds to an exothermic process in the DSC curve, so it can be assigned to the decomposition of copper acetate and release of carbon dioxide. The small mass losses detected at temperatures above 600 °C could be due to the combustion of carbonaceous remains produced during the decomposition of copper acetate. In Fig. 1B, corresponding to the catalyst prepared with copper nitrate, the second mass loss is observed between 230 ºC and 278 ºC, which could be originated by the decomposition of the nitrate generating the release of the corresponding oxides. Unlike what was observed with copper acetate, in the case of copper nitrate no evolution of heat is detected during its decomposition, probably due to the small heat of reaction that is expected for the decomposition of nitrate in air. For the catalyst prepared with copper sulfate (Fig. 1C), heat evolution up to 600 °C is not detected either. Regarding the TGA curve, a slight loss of mass is observed between 525 °C and 575 °C, and a more significant one at 610 °C. These mass losses at relatively high temperatures indicate a high thermal stability of the copper sulfate precursor (Alexandrescu *et al.*, 1995).

To complement the results of thermal analysis, FTIR spectroscopy measurements were made at the solids before and after calcination. Figure 2 also includes the spectra of the support silica and the precursor salts as references. Silica exhibits the typical bands of SiO_2 (Zhu *et al.*, 2015; Zhang *et al.*, 2012). Likewise, all the characteristic bands of SiO_2 are detected in the copper-bearing catalysts, although with a slight decrease in intensity, probably due to the copper-silica interaction. In the spectra of the uncalcined samples, absorption bands of the copper precursor salts are expected, and this is clearly observed in the spectrum of the sample obtained with copper nitrate, where the characteristic band of the nitrate group at 1384 cm^{-1} is present (Castro and Jagodzinski, 1991). This band disappears after calcining at 500 °C, corroborating the decomposition detected in the TGA tests. In the spectra of the catalysts prepared with copper acetate and copper sulfate, the bands corresponding to the precursors are not detected. In the case of sulfate, the bands appear in the same region where silica exhibits strong Si-O-Si bond signals, so it is difficult to detect sulfate ion bands. In the case of acetate, the absence of signals could be due to a very low concentration of acetate ions on the silica surface. On the other hand, regarding the copper species present in the catalysts, the FTIR spectra do not provide information, since no new signals attributable to copper species are detected, probably due to overlapping with the SiO_2 signals.

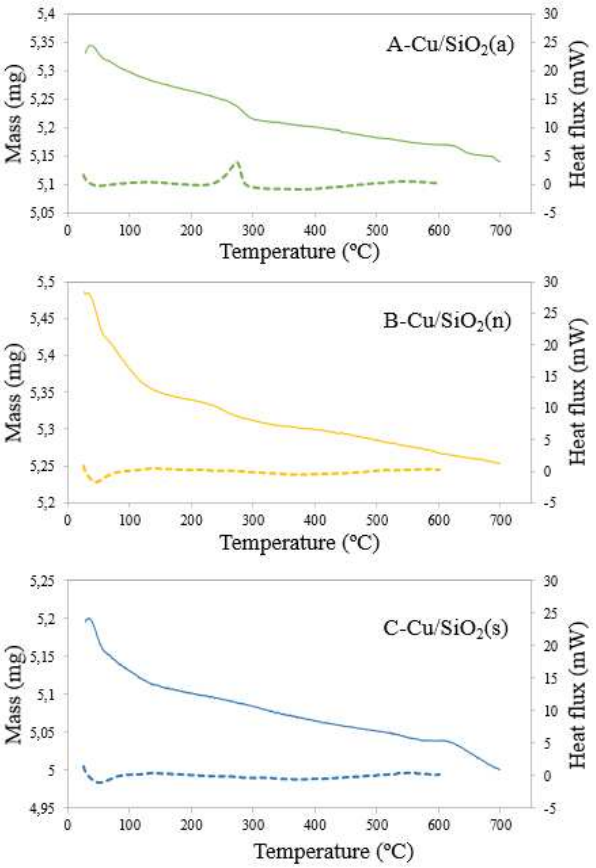

Figure 1: Results of TGA (solid line) and DSC (dotted line).

In order to identify copper species, determinations by XRD were made. As can be seen in Fig. 3, they all show a broad signal centered at the value of 2θ=22°, which is characteristic of amorphous silica. Only in the diffractogram of $Cu/SiO_2(n)$ two weak signals are detected at 2θ = 35.5° and 38.7° that correspond to the most intense diffraction lines of CuO monoclinic. In the diffractograms

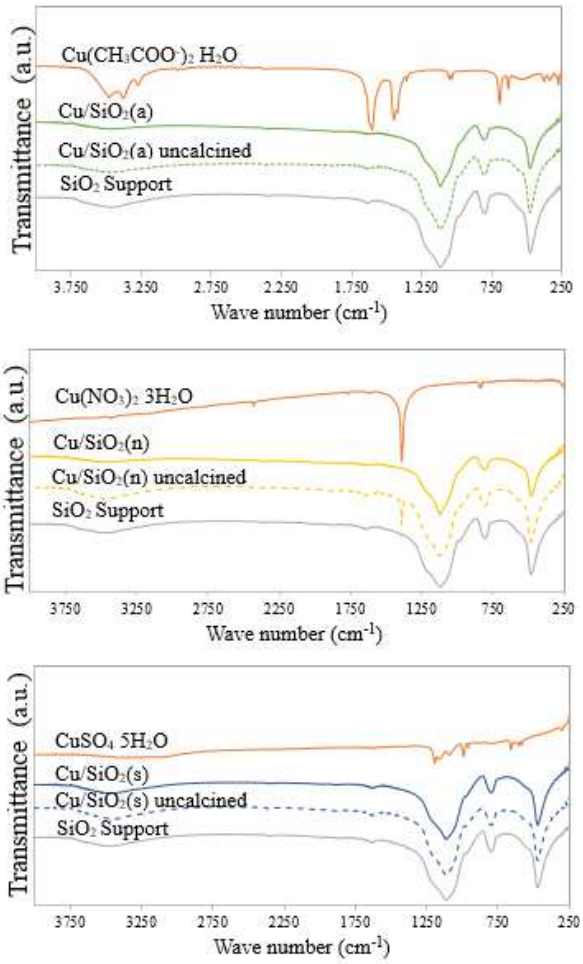

Figure 2: FTIR spectra of the precursor reagents, the silica support and the catalysts before and after calcination.

of $Cu/SiO_2(a)$ and $Cu/SiO_2(s)$, no other lines corresponding to phases containing copper are evident. This could be due to low concentration of copper species, to the formation of particles smaller than 4 nm, or to the formation of an amorphous phase.

Atomic absorption spectroscopy (AAS) analyses were performed to determine the copper content present in the catalysts. As can be seen in Table 1, the catalysts prepared with nitrate and sulfate contain less than 1% w/w copper, while the catalyst prepared with copper acetate contains almost twice as much. Relating these results with those of XRD, it can be deduced that the absence of diffraction peaks in $Cu/SiO_2(s)$ could be due to the low copper content. In contrast, the lack of XRD signals in $Cu/SiO_2(a)$ would be due to the formation of an amorphous or nanometric copper oxide phase, probably highly dispersed on the silica surface. For $Cu/SiO_2(n)$, the copper content is below 1% w/w, but despite this, CuO signals are detected, so it can be inferred that this oxide would have an average crystal size enough large to be detected.

The remarkable difference in copper concentration in the sample prepared with acetate with respect to those prepared with nitrate and sulfate is explained by the different pH of the solutions of those precursor salts. The

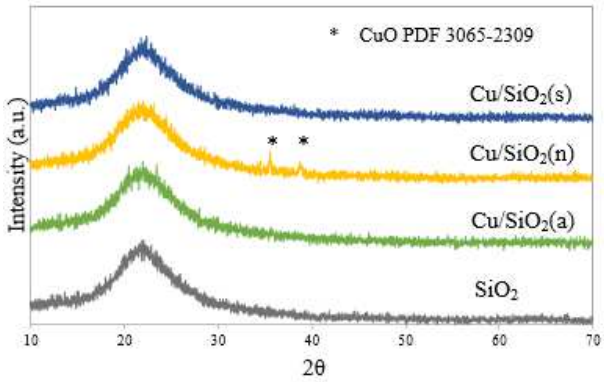

Figure 3: XRD of the catalysts.

Table 1: Cu content determined by AAS and H_2/Cu ratio from TPR.

Catalyst	Cu (% w/w)	H_2/Cu
$Cu/SiO_2(a)$	1.38	0.97
$Cu/SiO_2(n)$	0.72	1.05
$Cu/SiO_2(s)$	0.79	2.86

0.2 M nitrate and sulfate solutions presented a pH of 3.86 and 4.10, respectively; while the 0.2 M copper acetate solution had a pH of 5.33. Bearing in mind that the cation adsorption method used to prepare the catalysts relies on the electrostatic interaction of Cu^{2+} cations with the surface charges of the support silica, it is important to consider the difference between the point of zero charge (PZC) of silica and the pH of the solution containing the copper ions (Munnik *et al*, 2015). In the case of silica, it has been reported that the value of PZC is around 2 (Mustafa *et al.*, 2002). Therefore, the higher the pH of the solution of copper salts, the greater the difference with the PZC of silica. Furthermore, taking into account that the silica surface is negatively charged at pH above PZC, greater density of charged surface hydroxyl groups is expected when the solution pH increases. In conclusion, the higher the pH of the solution of copper salts, the greater the electrostatic adsorption of Cu^{2+} ions. So, the relationship between the pH of the solutions and the amount of copper present in the catalysts corresponds exactly to the preceding analysis.

The observations by means of SEM indicate that there are no significant morphological changes in the silica support after the addition of the active phase. In Fig. 4, SEM images of typical catalyst particles alongside EDS spectrum are shown. Copper is detected in all catalysts, but the quantification is not reliable since the copper amount is close to the detection limit. A relevant result of microanalysis by EDS is the presence of sulfur (1.13 % w/w) in the $Cu/SiO_2(s)$ catalyst.

Another interesting observation is the formation of a "star" shaped phase, in some of the SEM images of the $Cu/SiO_2(n)$ catalyst (Fig. 5). Analyzing the composition by EDS, an elevated copper content was determined, so it can be assumed that the phase is formed by the copper oxide taking as growth nucleus a silica particle. The large particle size shown by this phase would explain the appearance of the CuO diffraction lines even when the copper content is lower than 1% w/w. The textural charac-

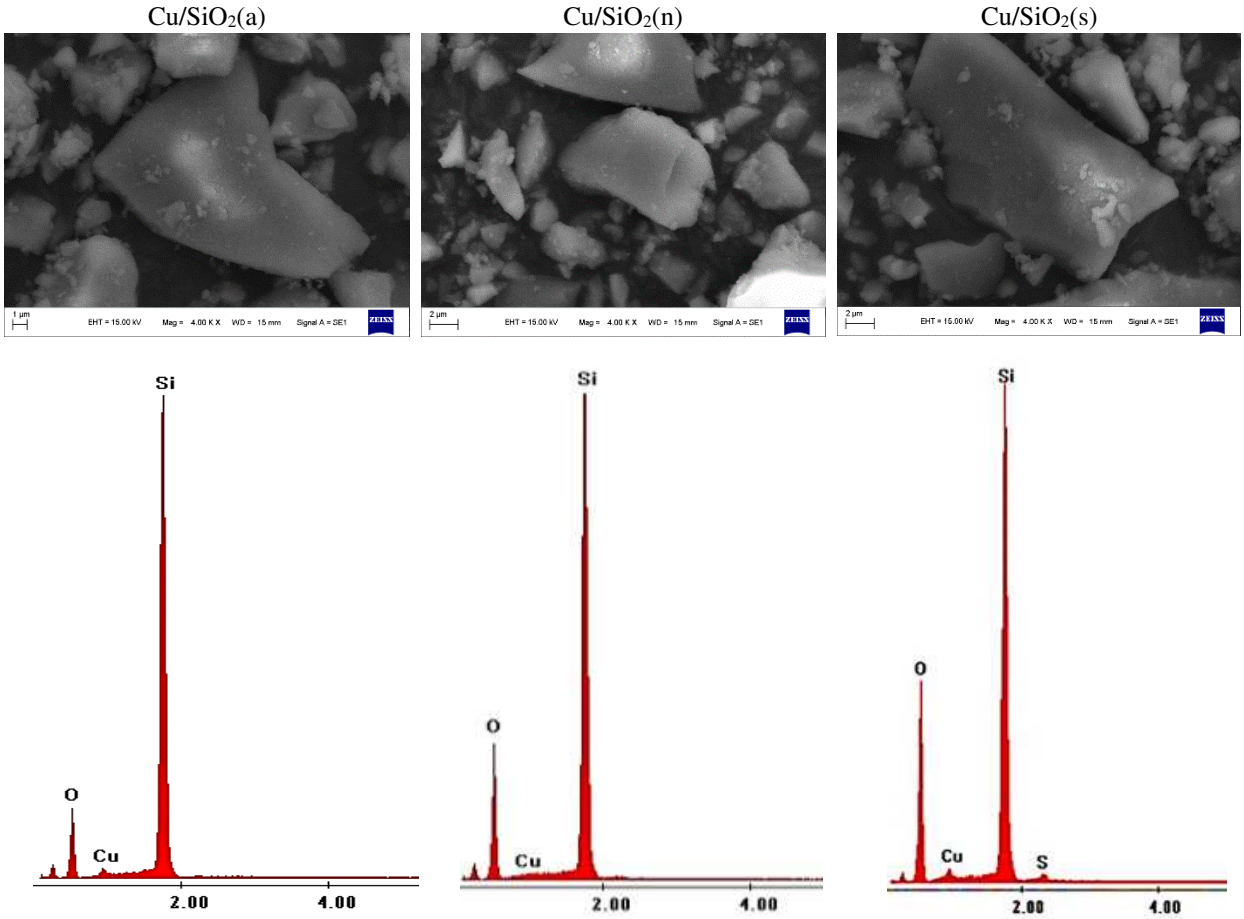

Figure 4: SEM image of the catalysts (above) and EDS spectra (below).

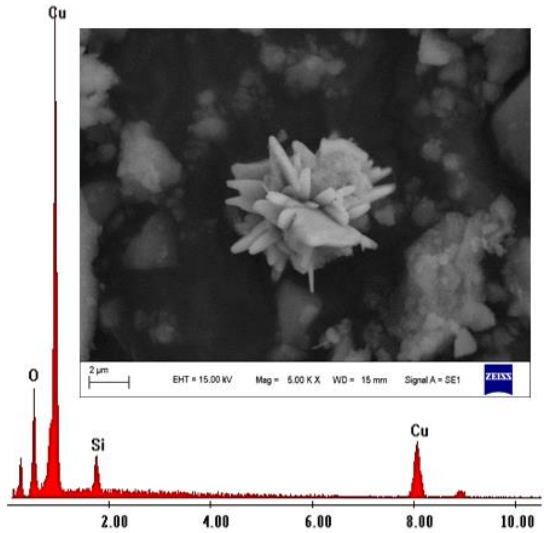

Figure 5: SEM image of the phase formed on the $Cu/SiO_2(n)$ catalyst and EDS spectrum.

teristics were analyzed from the isotherms of nitrogen adsorption-desorption. In Table 2, the specific surface area by BET method (S_{BET}), the pore volume (V_{pore}) and pore mean size (D_{pore}) are presented. As can be observed, the S_{BET} of $Cu/SiO_2(a)$ and $Cu/SiO_2(s)$ are 10% and 2.5% lower than that of SiO_2 used as support, respectively. Instead, the S_{BET} of $Cu/SiO_2(n)$ shows an increase of 12%. This S_{BET} increase could be due to the formation of the crystalline CuO on the SiO_2 surface, while the S_{BET} decrease is associated to surface coverage and pore blocking by the copper oxide species, in agreement with the results of pore volume and pore size, particularly for the $Cu/SiO_2(a)$ catalyst.

To complete the characterization of the catalysts, temperature programmed reduction (TPR) measurements were performed. It is worth noting that this technique allows to deduce the nature of the active phase and possible interactions between the active phase and the support. The reduction profiles of the catalysts show a single reduction peak (Fig. 6), whose maximum is located at different temperatures. When comparing the reduction curves, it is evident that the copper present in the $Cu/SiO_2(n)$ catalyst begins its reduction at the same temperature as the bulk CuO used as reference, but the peak

Table 2. Textural characteristics of the support and catalysts.

Catalyst	S_{BET} (m^2/g)	V_{pore} (cm^3/g)	D_{pore} (Å)
SiO_2	122	0.23	58
$Cu/SiO_2(a)$	110	0.21	55
$Cu/SiO_2(n)$	137	0.26	59
$Cu/SiO_2(s)$	119	0.23	58

maximum is to higher temperature indicating a strong interaction of copper oxide with the silica (Santori *et al.*, 2000). This result is in line with the bulk copper oxide formation detected by XRD and observed in the SEM images. In contrast, the reduction peaks of Cu/SiO_2(a) and Cu/SiO_2(s) appear at lower temperature than the reference CuO. According to reported in bibliography (Van Der Grift *et al*, 1990); the small copper oxide particles highly dispersed on the surface of the support silica are reduced at lower temperature than the bulk CuO. This information is in good agreement with the absence of diffraction lines in XRD.

Additional information from TPR can be obtained calculating the hydrogen consumption during the reduction of the catalysts. For this, the bulk CuO reduction curve was used as a calibration point. The results, expressed as moles of hydrogen per copper atom (H_2/Cu), are presented in Table 1. It is well known that copper forms oxidized species in +2 oxidation state when calcined in air. Therefore, according to Eq. 1

$$CuO + H_2 \rightarrow Cu^0 + H_2O, \qquad (1)$$

a value of H_2/Cu ratio approximately equal to 1 is expected. For the Cu/SiO_2(a) and Cu/SiO_2(n) catalysts this ratio is verified within an experimental error of ±5%, but for the Cu/SiO_2(s) catalyst, the H_2/Cu ratio is abnormally high. This could be due to the presence of other reducible species besides copper, or else, to the release of gases interfering with the signal of the thermal conductivity detector. To corroborate this, the Cu/SiO_2(s) sample was reduced under the same conditions as the first time, and subsequently, an *in situ* oxidation in air flow was carried out to obtain the copper oxide. Once the sample was cooled, it was again reduced. As can be observed in Fig. 6, the peak of the second reduction is very different from that of the first one. Also, the H_2/Cu ratio during the second reduction was 1.03, thereby confirming that in the first reduction there is a signal interference produced by gas release. It is worth commenting that in the TGA assays no appreciable mass loss was detected below 500 °C (calcination temperature during catalyst preparation), but a mass loss above 610° C was observed. It is highly likely that the decomposition of these species under TPR conditions occurs more easily than in air atmosphere. In fact, during the second reduction these species are no longer present, and only the reduction signal of copper oxide species dispersed on the silica is detected. The residual species would be originated from the precursor salt (copper sulfate), since in the EDS spectrum of the Cu/SiO_2(s) catalyst a small amount of sulfur was detected.

VI. CONCLUSIONS

The joint interpretation of the results allows to deduce that the copper acetate precursor decomposes during catalyst preparation generating nanosized copper oxide species highly dispersed on the silica surface, whereas the copper nitrate precursor leads to the formation of bulk-type copper oxide strongly interacting with the support silica and the copper sulfate precursor is not completelydecomposed during the preparation of the catalyst. The highest copper content was obtained with the acetate precursor, due to lower acidity of its solution, which generates a higher negative charge density on the silica surface and higher affinity for the cupric ions. In general terms, the great influence of the nature of the precursor salt on the physicochemical characteristics of silica-supported copper catalysts prepared by the method of cationic adsorption is established. Depending on the application intended for these catalysts, one or another physicochemical characteristic can be achieved through appropriate selection of the precursor salt, as demonstrated in this work.

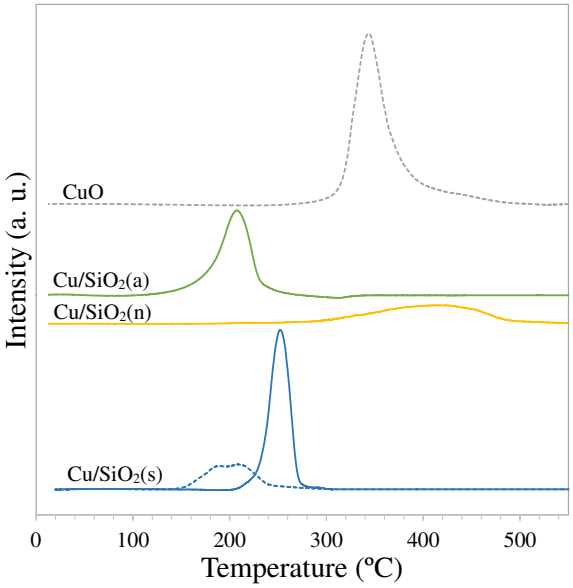

Figure 6: TPR curves of the catalysts and cupric oxide. For Cu/SiO_2(s), dotted line corresponds to second reduction.

ACKNOWLEDGEMENTS

The authors thank the financial support from UNSL, CONICET and FONCYT-ANPCyT of Argentina. Special thanks are due to INTEQUI technical staff (M. G. Amaya, M. E. Fixman, M. M. Barroso Quiroga, and J. Rigau) for their collaboration during the acquisition of some experimental data.

REFERENCES

Aubrecht, J., Kikhtyanin, O., Pospelova, V., Paterová, I., Kubička, D., Zaccheria, F., Scotti, N., Ravasiod N. (2022) Enhanced activity of Cu/SiO_2 and Cu/ZrO_2 catalysts in dimethyl adipate hydrogenolysis, *Catal. Today*. In Press.

Alexandrescu, R., Popescu, C., Morjan, I., Voicu, I. and Dumitras, D.C. (1995) IR laser chemical processing of metal salts for preparation of oxides and metal-containing layers. *Infrared Phys. Technol*. **36**, 1–13.

Castro, P.M. and Jagodzinski, P.W. (1991) FTIR and Raman spectra and structure of $Cu(NO_3)^+$ in aqueous solution and acetone, *Spectrochim. Acta Part A: Mol. Spectrosc.* **47**, 1707–1720.

Guerreiro, E.D., Gorriz, O.F., Larsen, G. and Arrúa, L.A. (2000) Cu/SiO_2 catalysts for methanol to methyl formate dehydrogenation. A comparative study using different preparation techniques. *Appl.*

Catal. A Gen. **204**, 33–48.

Hossain, S.T., Almesned, Y., Zhang, K., Zell, E.T., Bernard, D.T., Balaz, S. and Wang, R. (2018) Support structure effect on CO oxidation: A comparative study on SiO_2 nanospheres and CeO_2 nanorods supported CuO_x catalysts. *Appl. Surf. Sci.* **428**, 598–608.

Huang, L., Lin, L., Chen, C., Ye, R., Zhu, L., Yang, J., Qin, Y., Cheng, J. and Yao, Y. (2022) β-Cyclodextrin promoted the formation of copper phyllosilicate on Cu-SiO_2 microspheres catalysts to enhance the low-temperature hydrogenation of dimethyl oxalate. *J. Catal.* **413,** 943-955.

Martinez, A.A., Fixman, E.M., Cánepa, A.L. and Barbero, B.P. (2020) Preparation, characterization, and application of nano-FeOx/Al_2O_3/cordierite monolithic catalysts for heterogeneous dark-Fenton reaction, *J. Chem. Technol. Biotechnol*. **95,** 2868-2878.

Munnik, P., De Jongh, P.E. and De Jong, K.P. (2015) Recent developments in the synthesis of supported catalysts, *Chem. Rev.* **115**, 6687–6718.

Mustafa, S., Dilara, B., Nargis, K., Naeem, A. and Shahida, P. (2002) Surface properties of the mixed oxides of iron and silica. *Colloids Surfaces A Physicochem. Eng. Asp.* **205**, 273–282.

Santori, G.F., Lladó, M.L., Siri, G.J., Casella, M.L. and Ferretti, O.A. (2000) Cu and CuSn supported catalysts for selective hydrogenation of cinnamaldehyde. *Lat. Am. Appl. Res.* **30**, 55 – 59.

Toupance, T., Kermarec, M. and Louis, C. (2000) Metal particle size in silica-supported copper catalysts. Influence of the conditions of preparation and of thermal pretreatments. *J. Phys. Chem. B*. **104**, 965–972.

Toupance, T., Kermarec, M., Lambert, J.F. and Louis, C. (2002) Conditions of formation of copper phyllosilicates in silica-supported copper catalysts prepared by selective adsorption. *J. Phys. Chem. B*. **106**, 2277–2286.

Van Der Grift, C.J.G., Mulder, A. and Geus, J.W. (1990) Characterization of silica-supported copper catalysts by means of temperature-programmed reduction. *Appl. Catal.* **60**, 181–192.

Wang, Z., Liu, Q., Yu, J., Wu, T. and Wang, G. (2003) Surface structure and catalytic behavior of silica-supported copper catalysts prepared by impregnation and sol-gel methods. *Appl. Catal. A Gen.* **239**, 87–94.

Xi, X., Ma, S., Chen, J. F. and Zhang, Y. (2014) Promotional effects of Ce, Mn and Fe oxides on CuO/SiO_2 catalysts for CO oxidation. *J. Environ. Chem. Eng*. **2**, 1011–1017.

Zhang, B. Hui S., Zhang S., Ji Y., Li W. and Fang D. (2012) Effect of copper loading on texture, structure and catalytic performance of Cu/SiO_2 catalyst for hydrogenation of dimethyl oxalate to ethylene glycol, *J. Nat. Gas Chem.* **21**, 563–570.

Zhong, X., Barbier, J., Duprez, D., Zhang, H. and Royer, S. (2012) Modulating the copper oxide morphology and accessibility by using micro-/mesoporous SBA-15 structures as host support: Effect on the activity for the CWPO of phenol reaction. *Appl. Catal. B Environ.* **121–122**, 123–134.

Zhu, S., Gao, X., Zhu, Y., Fan, W., Wang, F. (2015) A highly efficient and robust Cu/SiO_2 catalyst prepared by the ammonia evaporation hydrothermal method for glycerol hydrogenolysis to 1,2-propanediol, *Catal. Sci. Technol.* **5**, 1169–1180.

Received: August 4, 2022
Sent to Subject Editor: August 29, 2022
Accepted: October 12, 2022
Recommended by Subject Editor Laura Briand